Supporting Information

Stojanov et al. 10.1073/pnas.1103681108

SI Materials and Methods

Patients and Controls. All PFAPA (the syndrome of periodic fever associated with aphthous stomatitis, pharyngitis, and cervical adenitis) and hereditary periodic fevers (HPF) patients were enrolled in an Institutional Review Board-approved protocol of the National Institute of Arthritis and Musculoskeletal and Skin Diseases (NIAMS). PFAPA patients were also referred to NIAMS from the University of Connecticut Health Sciences Center/Connecticut Children's Medical Center (Hartford, CT) and the Department of Pediatrics, Vanderbilt University School of Medicine (Nashville, TN). The healthy controls were enrolled at NIAMS and the Nemours A.I. duPont Hospital for Children (Wilmington, DE). Written informed consent was provided by the parents or legal guardians of all patients and controls.

As the majority of PFAPA patients were Caucasians; we only included Caucasian patients and controls to ensure that the laboratory results were not influenced by differences in ethnicity. The control population consisted of two groups: 21 anonymized healthy children (12 females, 9 males; median age 10.8 y, range 4.9–14.5) with no history of acute infections or inflammatory conditions, and 12 children (seven females, five males; median age 7.4 y, range 1.8–16.2) with a genetically confirmed HPF during a disease flare (Fig. 1*B*). For microarray analysis, six healthy controls were matched with PFAPA patients for age (within median 1.8 y of patient ages, range 0.4–5) and sex, and six pediatric HPF patients during a flare (three females, three males; median age 5 y, range 1.8–16.2) were analyzed.

Collection and Analysis of Blood Samples. Blood samples were collected and tested for complete blood cell counts, C-reactive protein, serum cytokines, and global gene expression analyses in patients and in controls. Serum immunoglobulins (IgG, IgM, IgA, IgE and IgD), antinuclear antibody, antistreptolysin O, anti-DNaseB, antibody titers against HSV 1 and 2, EBV, and CMV, liver and kidney function tests, and urinanalysis were tested in patients at the time of study enrollment. Circulating lymphocyte phenotyping was performed in patients and healthy controls. Serum complement components (CH50, AH50, Properdin Factor B, C1q, C2, C3, C4, C5, C1 esterase inhibitor complement antigen) were measured in patients and HPF controls. DNA sequence analysis for HPF mutations was performed in patients and controls at study enrollment. Plasma complement activation fragments (Bb, C3a, C4D, and C5a) were measured in patients. Except for the serum complement measurements, which were performed at the Mayo Clinic (Rochester, MN), and the plasma complement fragments, which were determined at National Jewish Health (Denver, CO), all analyses were performed at the National Institutes of Health.

DNA Sequence Analysis. DNA sequence analysis for HPF mutations was performed in patients and controls at study enrollment. Genomic DNA was isolated from peripheral blood leukocytes using the Gentra Puregene Blood Kit (Qiagen) according to the manufacturer's instructions. Sequence analysis was performed of exons 8 and 10 of *MVK*, exons 2, 3, and 10 of *MEFV*, exons 2 to 5, as well as introns 2 and 4 of *TNFRSF1A*, five overlapping fragments of exon 3 of *CIAS1*, and exons 1 to 5 of *ELA2*.

Microarray Analysis. RNA was extracted from whole peripheral blood collected in PAXgene tubes (Qiagen) according to the manufacturer's instructions, and RNA integrity was assessed by using an Agilent 2100 Bioanalyzer (Agilent Technologies). Total RNA was transcribed to labeled cDNA using the Ovation Whole Blood Solution (NuGen). The biotinylated cDNA was hybridized to the Affymetrix GeneChip HG-U133A 2.0 Array (Affymetrix) and detected according to the manufacturer's standard protocols. Arrays were scanned using an Affymetrix GeneChip Scanner 3000. Raw microarray data are available at the Gene Expression Omnibus Web site (www.ncbi.nlm.nih.gov/geo/) under accession number GSE17732.

Affymetrix probe data were screened for quality and array comparability by using control metrics including background, noise, 5′ to 3′ ratios of housekeeping genes, percent of genes called present, and scale factor. Raw intensity data were converted to .CEL and Metrics files, respectively, using Affymetrix GeneChip Operating Software (GCOS v1.4). To control for chip-to-chip variation, gene-expression values were generated using the Robust Multichip Array algorithm (1) as implemented in Microarray Data Management and Analysis System (MDMAS), a software developed at NIAMS. Only transcripts identified as "present" by the Microarray Suite software, version 5 (MAS 5.0) (Affymetrix) in at least four of the six samples of each group were analyzed to filter for reliable intensity measurements from each individual chip. Statistical gene-expression comparisons were performed in MDMAS using paired *t* test or Welch's approximate *t* test for paired (PFAPA flare vs. nonflare) or unpaired group comparisons.

To establish stringent criteria for our comparison of paired PFAPA samples during and between episodes, we chose a fold-change of two or greater and a false-discovery rate (FDR) of 2%. On the other hand, when comparing unpaired samples from PFAPA and HPF patients during fever, we set the fold-change and FDR at 1.5 or greater and 20%, respectively, to maximize the possibility of detecting differentially expressed genes. Multiple probe sets for a single gene were eliminated by including only the probe with the largest fold-change. We carried out principal-component analysis using Partek software, version 6.3 (Partek Inc.). We used Ingenuity Pathways Analysis software (Ingenuity Systems) to identify biologic pathways encompassing our lists of differential expressed genes. Unsupervised hierarchical clustering of differentially expressed probe sets was performed to group genes by expression patterns using Pearson correlation (Partek Inc.).

Real-Time Quantitative RT-PCR. DNase treated whole blood RNA was converted to cDNA using the SuperScript III Platinum Two-Step qRT-PCR Kit (Invitrogen). Quantitative RT-PCR analysis was performed using TaqMan Gene Expression Assays, and an ABI Prism 7300 Sequence Detector (Applied Biosystems). Final quantification was derived using the comparative threshold cycle (C_t) method, as described by the manufacturer, with β_2-microglobulin serving as endogenous control. Data shown are respective gene expression relative to healthy controls. Efficiency of all primer sets was tested using a standard serial dilution of cDNA.

Listed below are human TaqMan Gene Expression Assays applied for qRT-PCR detection of indicated cytokines and factors (Applied Biosystems); the symbol of each target gene is followed by the product catalog number.

IL1B, Hs01555413_m1; *IL1RN*, Hs00893626_m1; *AIM2*, Hs00915711_m1; *CASP1*, Hs00354836_m1; *CASP5*, Hs00362078; *NLRP1*, Hs01049643_m1; *NLRP3*, Hs00366465_m1; *PYCARD (ASC)*, Hs00203118_m1; *CXCR3*, Hs00171041_m1; *STAT1*, Hs01014002_m1; *SERPING1*, Hs00934330_m1; *C1QB*, Hs00608019_m1; *C2*, Hs00918863_m1; *CD59*, Hs00174141_m1; *B2M*, 4326319E.

Cytokines and Chemokines. Blood samples for the measurement of cytokines were centrifuged (956 × *g* for 10 min) immediately after collection, and serum was stored at −80 °C until examined. Cytokine levels were determined by bead-based methods (BioRad Luminex) for assay of IL-1β, IL-1ra, IL-2, IL-4, IL-5, IL-6, IL-8, IL-9, IL-10, IL-12p70, IL-13, IL-15, IL-17, Eotaxin, FGF basic, G-CSF, GM-CSF, IFN-γ, IP-10, MIG, MCP-1, MIP-1α, MIP-1β, PDGF bb, RANTES, TNF-α, and VEGF; and enzyme-linked immunosorbent kit (Medical & Biological Laboratories Co.) for assay of IL-18.

Flow Cytometry Analysis for Lymphocyte Phenotyping. EDTA anticoagulated peripheral-blood specimens were processed within 48 h after sampling using a whole-blood staining method as previously described (2). FITC, phycoerythrin, peridinin-chlorophyll-protein, or allophycocyanin were used as fluorophores. T cells and T-cell subsets were identified by staining with anti-CD3, anti-CD4, anti-CD8, HLA-DR, CD25 (BD Biosciences), and anti-γ/δ TCR (Pierce-Endogen). B cells were evaluated with anti-CD20 (BD Biosciences) and natural killer cells with a combination of anti-CD16 and anti-CD56 (BD Biosciences) on $CD3^+$ or $CD3^-$ lymphocytes. Mouse IgG1 (BD Biosciences) was used as isotype control. Lymphocytes were identified on a gate established by forward and side-angle scatter, and confirmed using anti-CD45/-CD14 (Leukogate; BD Biosciences). The absolute number of each lymphocyte subset was calculated by multiplying the percentage of cells staining positively by the absolute peripheral blood lymphocyte count. Analysis was carried out on a FACSCalibur (BD Biosciences) flow cytometer with CellQuest software (BD Biosciences).

Complement System Analyses. Serum and plasma samples were separated immediately after blood sampling and kept at −80 °C until measurement. The total hemolytic complement assay (CH50) and the AH50 assay were used as screening methods to detect abnormalities in the activation of the classic and alternative pathway, respectively. Analyses were performed in sera as previously reported (3, 4). Reference values were 30 to 75 U/mL for CH50 and 75 to 170% normal for AH50. In sera complement levels were determined by radial immunodiffusion for assay of Properdin Factor B (normal 18–46 mg/dL) and C2 (normal 1.1–3.0 mg/dL), by nephelometry assays for analysis of C1q (normal 12–22 mg/dL), C3 (normal 90–180 mg/dL), C4 (normal 10–40 mg/dL), C5 (normal 7.4–11.7 mg/dL), and C1 esterase inhibitor complement antigen (normal 19–37 mg/dL). Plasma levels of complement activation fragments were measured using ELISA kits that detect Bb (normal 0.35–0.85 UG/ML), and C4D (normal 0.52–7.88 μg/mL), and by radial immunodiffusion for assay of C3a (normal 0–940 ng/mL), and C5a (normal 4.7–9.5 ng/mL).

Statistical Analysis. If not stated otherwise, we applied the two-tailed Wilcoxon signed-rank test or Mann-Whitney *U* test for paired (PFAPA flare vs. nonflare) or unpaired group comparisons, respectively. *P* values < 0.05 indicated statistical significance. We calculated correlations using Spearman's correlation coefficient. We used a series of multivariate logistic regression models to examine the independent associations of different cytokines, chemokines, and leukocyte subsets with flare vs. nonflare status. To determine whether changes in cytokines and chemokines from flare to nonflare status were interrelated, we used multivariate linear regression. Analysis was performed using SPSS 14.0 for Windows.

Statistical Analysis (Multivariate Logistic Regression Analysis) for Identification of Flare Predictors. We used each of the six cytokines/chemokines as an independent variable in each model. In separate models, we then added other cytokine and chemokine measures as a second independent variable. Because of the small number of subjects, we limited the regression models to two independent variables. In each model, we tested if the cytokine/chemokine was significantly associated with flare status independent of the other measure. If the addition of the second independent variable to the model resulted in the tested cytokine/chemokine levels not to be significantly associated with flare status and the second variable was significantly associated with flare status, this was evidence that the second variable mediated the association between the tested cytokine/chemokine levels and flares.

SI Results

In Vivo Analysis of Inflammatory and Antimicrobial Protein Measures. Six of 21 (29%) of our PFAPA patients showed mildly elevated antinuclear antibody titers between ≥1 and <3 EU (norm <1 EU), which are not considered to be indicative for an autoimmune disease. Three (14%) and four (19%) of our patients had elevated levels of antistreptolysin O and anti-DNaseB, respectively. None of our PFAPA patients had signs of a current or past herpes simplex type 1 or 2 infections, whereas four (19%) children presented positive EBV-IgG titers, with three of them being positive for EBNA-IgG and one patient was in addition positive for CMV-IgG. None of the PFAPA patients had virus-specific IgM titers.

1. Irizarry RA, et al. (2003) Summaries of Affymetrix GeneChip probe level data. *Nucleic Acids Res* 31:e15.
2. Uzel G, et al. (2008) Reversion mutations in patients with leukocyte adhesion deficiency type-1 (LAD-1). *Blood* 111:209–218.
3. Yamamoto S, et al. (1995) Automated homogeneous liposome-based assay system for total complement activity. *Clin Chem* 41:586–590.
4. Platts-Mills TA, Ishizaka K (1974) Activation of the alternate pathway of human complements by rabbit cells. *J Immunol* 113:348–358.

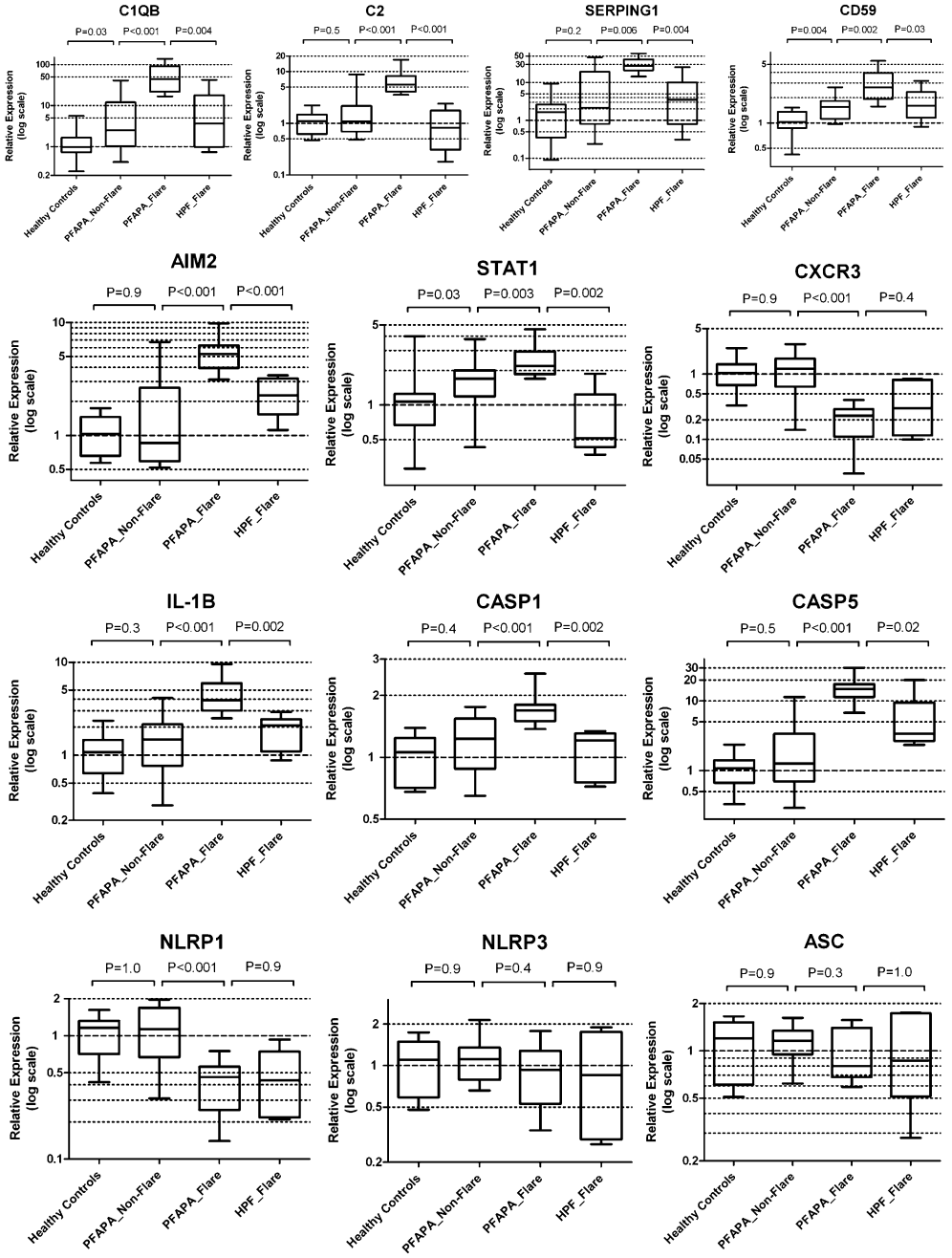

Fig. S1. Validation of microarray-based innate immune gene expression signatures in a larger group of PFAPA patients and controls. RNA transcript levels were measured in whole-blood samples by means of qRT-PCR in 15 paired PFAPA samples (active and inactive disease state), 11 healthy controls, and 6 flare samples of patients with hereditary periodic fevers [two familial Mediterranean fever (M694V/E148Q and M694del in *MEFV*), one TNF receptor-associated periodic syndrome (C52G in *TNFRSF1A*), three cryopyrin-associated periodic syndromes (two G569R, and L632F in *CIAS1*)]. The RNA transcript levels are expressed on a log (base-10) scale relative to the mean expression of transcripts from healthy controls. Boxes show relative expression values between the 25th and 75th percentiles; whiskers indicate the highest and lowest values for each group; horizontal lines within boxes represent median values.

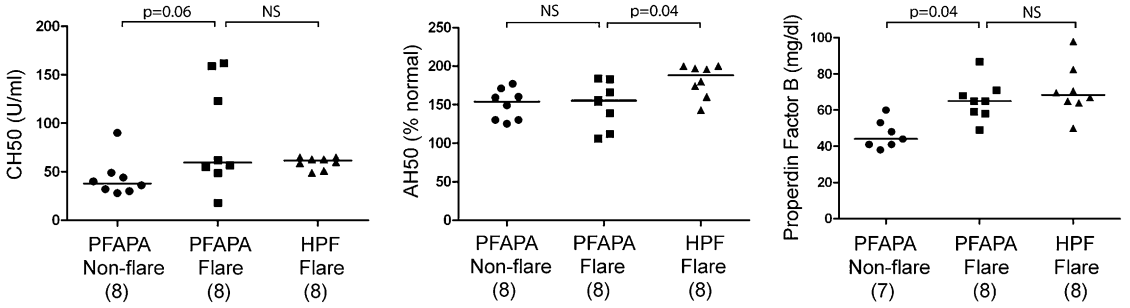

Fig. S2. Values of complement activity in PFAPA patients during and between flares, healthy controls, and HPF patients during flare.

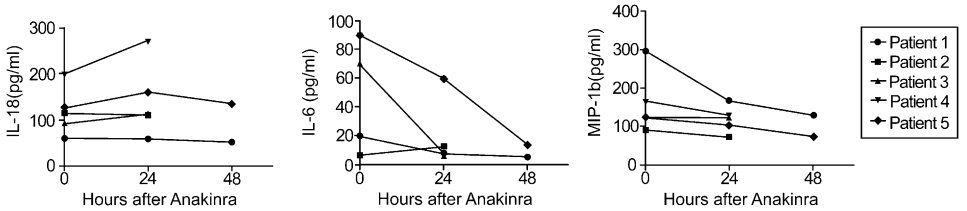

Fig. S3. Cytokine/chemokine measurements in sera before and after injection of anakinra.

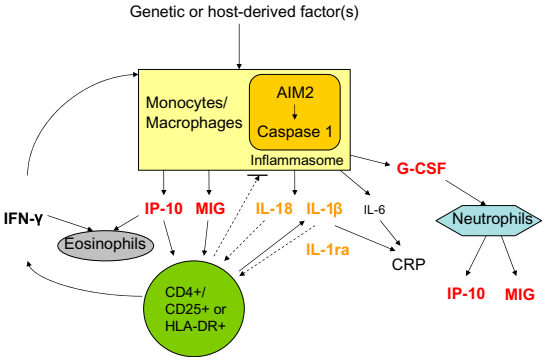

Fig. S4. Proposed pathogenic mechanism of PFAPA syndrome. Microbial colonization, possibly in the context of inherited or acquired immune abnormalities in the host, may trigger episodes of PFAPA via activation of mainly the classic complement cascade or—in case of dsDNA such as adenovirus—direct activation of the AIM2 inflammasome in monocytes/macrophages. Subsequent IL-1β/-18 secretion leads to fever and, in conjunction with IL-6, to an increase of acute-phase parameters, such as C-reactive protein. In parallel, IL-1β/-18 activate via their costimulatory effect local T lymphocytes, which secrete IFN-γ and signal back to monocytes/macrophages. These cells then increase their production of the IFN-inducible chemokines IP-10/CXCL10 and Mig/CXCL9, as well as G-CSF, which then recruit activated T lymphocytes, eosinophils, and neutrophils, respectively, to the local sites of inflammation as pharynx, adenoids, and cervical lymph nodes. Monocytes and activated T lymphocytes counteract the complement activation via secretion of soluble (C1-INH) and up-regulation of membrane-bound (CD59) inhibitors, respectively. The IL-1R antagonist, anakinra, blocks IL-1β effects, including perpetuation of the costimulatory T lymphocyte activity and downstream effects on Th1 chemokines. Solid arrows indicate a direct effect, dashed arrows indicate an indirect effect; chemokines/cytokines marked in red indicate the strongest PFAPA flare correlators, those marked in yellow indicate cytokines of the IL-1/-18 family, which, based on patients' response to anakinra, appear to drive the PFAPA flares.

Table S1. PFAPA flare-associated changes

Measure	Healthy control	*P* value*	PFAPA-patient nonflare	*P* value†	PFAPA-patient flare	*P* value‡	HPF-patient flare§
Complete blood cell count							
Leukocytes (k/μL)	6.5 (5.7–7.9)	0.4	7.1 (5.6–8.6)	<0.001	12.9 (9.8–15.4)	0.2	15 (11.8–18.7)
Absolute neutrophil count (k/μL)	3.1 (2.2–3.8)	0.6	2.9 (2.5–3.2)	<0.001	9.3 (6–11.1)	0.8	10.4 (6.6–12)
Absolute lymphocyte count (k/μL)	3 (2.5–3.3)	0.3	2.9 (2.6–4.5)	0.006	2.2 (1.7–3)	0.05	3.2 (2.2–5.1)
Absolute monocyte count (k/μL)	0.5 (0.4–0.54)	0.4	0.5 (0.45–0.62)	<0.001	1.2 (0.83–1.54)	0.04	0.87 (0.69–0.93)
Absolute eosinophil count (k/μL)	0.11 (0.09–0.21)	0.5	0.17 (0.11–0.21)	0.03	0.03 (0.0–0.04)	0.007	0.2 (0.04–0.62)
Absolute basophil count (k/μL)	0.04 (0.0–0.07)	1.0	0.02 (0.0–0.07)	0.8	0.03 (0.0–0.07)	0.2	0.05 (0.03–0.10)
Hemoglobin (g/dL)	13.2 (12.6–13.8)	0.002	12.3 (11.8–12.8)	0.4	12.3 (11.6–12.9)	0.02	11.1 (9.9–12.0)
Platelets (k/μL)	287 (256.5–334.5)	0.3	346 (251–374.8)	0.02	269 (213–345)	0.02	345 (298–509)
Circulating lymphocyte subpopulations							
CD3 (/μL)	2,161 (1,936–2,434)	0.4	2,273 (1,929–3,402)	0.002	1,495 (1,236–2,053)	NA	ND
CD3/CD4 (/μL)	1,127 (1,045–1,481)	0.9	1,988 (964–1,988)	<0.001	813 (622–1,191)	NA	ND
CD3/CD8 (/μL)	718 (604–887.5)	0.3	780 (700–1,121)	0.003	506 (341.5–702.5)	NA	ND
Double negative CD3 (/μL)	186 (133–234)	0.2	221 (135–316)	0.02	142 (78.5–196.5)	NA	ND
CD3/γ/δ (/μL)	158 (122–243)	0.02	242 (170–333)	0.2	169.5 (98–284.5)	NA	ND
CD4/HLA-DR (/μL)	81 (64–93.5)	0.4	70 (44–90)	0.03	51 (31.5–65.5)	NA	ND
CD4/CD25 (/μL)	360 (323.5–481.5)	0.07	320 (215–458)	0.004	211 (187.5–310.5)	NA	ND
CD8/HLA-DR (/μL)	100 (76–169)	0.8	106 (67–179)	0.3	94 (56–167)	NA	ND
CD8/CD25 (/μL)	85 (60.5–132.5)	0.4	70 (59–102)	0.7	70 (45–97)	NA	ND
CD20 (/μL)	393 (313–529)	0.5	451 (294–644)	0.3	415 (322.5–502.5)	NA	ND
($CD16^+$ or $CD56^+$)/CD3- (/μL)	242 (132–371)	0.2	280 (210–448)	0.9	319 (218.5–422.5)	NA	ND
($CD16^+$ or $CD56^+$)/$CD3^+$ (/μL)	167 (120–257)	0.9	167 (113–265)	0.3	121 (93.5–196)	NA	ND

Data for Healthy Control, PFAPA-patient nonflare, PFAPA-patient flare, and HPF-patient flare represent median (25–75% percentile). Healthy Control, *n* = 21; PFAPA-patient nonflare, *n* = 19–21; PFAPA-patient flare, *n* = 16–19; HPF-patient flare, *n* = 9–10. NA, not applicable; ND, not done.

*Comparison of healthy controls vs. PFAPA-patient nonflare.

†Comparison of PFAPA-patient nonflare vs. PFAPA-patient flare.

‡Comparison of PFAPA-patient flare vs. HPF-patient flare.

§HPF diagnoses: two FMF (M694V/E148Q and M694del in *MEFV*), two TRAPS (C52G and C72R in *TNFRSF1A*), three HIDS (V377I/G171R and two V377I/I268T in *MVK*), four CAPS (two G569R, V262A, and L632F in *CIAS1*), and one PAPA (E250Q in *PSTPIP1*).

Dataset S1. Transcripts increased or decreased in whole-blood cells from PFAPA patients during flare compared with their asymptomatic interval

Dataset S1 (XLS)

Dataset S2. Transcripts up- or down-regulated in whole-blood cells from PFAPA patients during flare compared with flares of patients with HPF syndromes

Dataset S2 (XLS)

Dataset S3. Serum complement components measured during flares in PFAPA patients

Dataset S3 (XLS)

Dataset S4. Spearman's correlation coefficients of correlations between significantly changed serum levels of chemokines, cytokines, and C-reactive protein during flares in PFAPA patients

Dataset S4 (XLS)

Dataset S5. Multiple logistic regression analysis of significantly elevated serum concentrations of chemokines and cytokines during PFAPA flares

Dataset S5 (XLS)

The relatively low odds ratios reflect the small units of measure (pg/mL) for the various cytokines and chemokines.

Dataset S6. Multivariate linear regression analysis of changes in chemokines and cytokines that were significant PFAPA flare predictors

Dataset S6 (XLS)